A SIMILITUDE BASED APPROACH ON THE FINITE ELEMENT MODELISATION OF CIRCULAR DRAWBEADS BEHAVIOR

Duarte, E. N., enduarte@mecanica.ufu.br
Oliveira, S. A. G., sgoulart@mecanica.ufu.br
Universidade Federal de Uberlândia, Campus Sta. Mônica, Bloco 1M, Sala FEMEC-CIMNE, 38400-902, Uberlândia, Brazil.

Neamtu, L., laur@quantech.es
Quantech ATZ, Gran Capitán, 2-4, 08034, Barcelona, Spain

Weyler, R., rafael.weyler@upc.edu
Universitat Politècnica de Cataluña, C. Colom 1, 08222, Terrassa, Spain.

Abstract. *Drawbeads are very important devices to control the material flow into the die cavity in sheet metal forming, although excessive deformations may be produced. There are some disadvantages in their using, such as difficulties of adjustment during die try-outs for obtaining the actual Drawbead Restraining Force (DBRF). To solve these problems, to control the sheet flow into the die cavity efficiently and to reduce the number of die try-outs, which are very time consuming, sufficiently accurate drawbeads concepts are necessary. The aim of this paper is to understand the influence on the DBRF of two sets of their main design characteristics, namely, the geometrical and the material properties. For this purpose simulations with Finite Element (FE) models were designed by varying each one of these factors and maintaining constant the other geometric and material parameters. A similitude analysis was run to establish this comparison. The results were compared with Nine (1978) experimental databases for circular cross section drawbeads and the average of absolute error was approximately 5 % and, for the cases studied, the maximum error was about 10%. Predictions derived from this approach are adequate, in terms of precision, when compared with analytical and experimental results. For this reason, the approach was used to develop a study about DBRF evaluations and was accepted as a contribution by STAMPACK®, an explicit finite element code used to simulate the forming process.*

Keywords*: Drawbead, restraining force, finite element method, sheet metal forming*

1. INTRODUCTION

A conventional drawbead is a device which has a semi-cylindrical bead located on one binder face that fits into a die groove. The most widely used geometry of the drawbead cross section is circular, although rectangular, triangular, trapezoidal and unsymmetrical geometries are also employed. In the current work, only the circular geometry is being approached, (see Fig. 1).

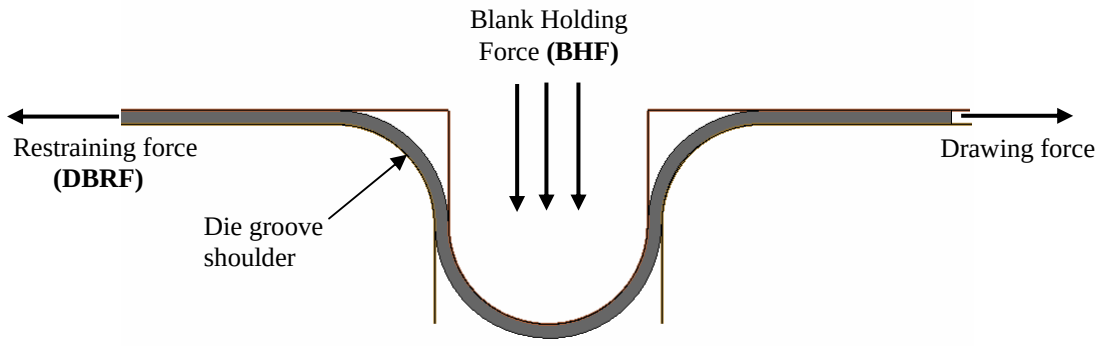

Fig.1. Drawbead in a stamping process with a circular cross section.

The improved quality of the parts obtained in sheet metal forming depends on the suitable control of the rate of material flow into the die cavity. This control is made by a restraining force supplied either by the blankholder, by the drawbeads or both. When the required restraining force is too high, the use of drawbeads is necessary, according Tufekci (1994). However, when the sheet passes through them, excessive deformations may be produced. Some others disadvantages, such as difficulties of adjustment during die try-outs in order to encounter the actual Drawbead Restraining Force (DBRF), may also occur.

In order to solve these problems and to reduce the number of die try-outs, which are very time consuming, precise drawbeads concepts are necessary. Thus, a study concerning the design of drawbeads in forming process must be performed in order to determine with accuracy the actual magnitude of this force.

The first analytical approach was done by Swift (1948). His work was carried out considering the bending and unbending succession when the sheet passes through the drawbeads. The material was assumed to be isotropic with linear strain-hardening and strain rate-independent behavior.

Nine (1978) performed experiments to study the influence of the bending deformation and friction on DBRF. These components have been separated and analyzed. Drawing and clamping load were measured for steel and aluminum sheets. His experimental data were discussed from the viewpoint of the materials effects which must be taken into account in a mathematical model for drawbead forces. In the present study, Nine's results were also used with a part of validation procedures.

Levy (1983) developed a semi-empirical procedure to establish a closed formula of DBRF. In his equation, parameters of material properties and geometries of the sheet and the drawbeads are considered. Using the Levy's model as a first approach, Stoughton (1988) developed an analytical formulation to predict the DBRF. The Stoughton's assumptions include Coulomb's law for friction, Hill's anisotropic yield criterion, rigid-plastic and with a rate-independent material behavior. The derivation of a closed formula was possible by integrating deformation work across the sheet thickness and along the full extension of the drawbead. His model is applicable to circular cross section beads, but has potential to be used with other geometrical forms.

Nowadays, there's a growing emphasis on Finite Element (FE) modeling in sheet metal forming. There's no doubt about the power of the numerical techniques. However, the three-dimensional (3D) FE simulation of complex parts forming has a high expensive computational cost. Thus, researches aiming to find solutions for this problem and to place these limitations to a more acceptable level are welcome. In one of these solutions, Carleer et al (1995) established an approach by which the distributions of DBRF of the sheet are initially curve-fitted as a function of displacement so that these functions are applied as boundary conditions to produce similar effects in the 3D modeling. This approach has been named the "equivalent drawbead method". Two-dimensional (2D) FE approaches to simulate the drawbeads have been therefore performed. Duarte (2005) developed a study, using the same approach, to investigate the influence of the sheet thickness on the DBRF.

The aim of this study is to understand the influence of the most important parameters describing the DBRF behavior. To this end, a hybrid approach was formulated using similitude with data bases developed using explicit based Finite Element (FE) simulations. This procedure was adopted after analyzing the good agreement between the 2D FE drawbead simulations carried out with STAMPAK ® and Nine's (1978) experimental results.

2. SIMILITUDE

The theory of similitude may be developed by dimensional analysis which involves consideration of the dimensions of the examined phenomenon. According to this theory special attention is focused on the conditions that would permit the behavior of two separated physical systems to be treated similarly. This theory allows the reduction of the number of involved quantities and a better analysis of the actual influence of dimensionless groups on the phenomenon under investigation.

Accurate prediction equations may be established when the dimensional analysis is combined with experimental procedures. Based on dimensional analysis, it is possible to formulate an equation which involves an unknown function of dimensionless groups, named π terms, which may be written, generically, as follows:

$$\pi_1 = F(\pi_2, \pi_3, \pi_4, ..., \pi_S) \tag{1}$$

where *s* represents the number of dimensionless groups – or π terms - involved in the phenomenon and may be obtained on the basis of the Buckingham π Theorem, see Murphy (1950). This theorem states that "the number of dimensionless and independent quantities required to express a relationship among the variables in any phenomenon is equal to the number of quantities involved minus the number of dimensions by which those quantities may be measured", that is:

$$s = n - b \tag{2}$$

in which, *s* represents the number of π terms, *n* the total number of quantities involved and b is the number of basic dimensions considered. Details may be found in Murphy (1950). Hypothetically, if there were eight quantities and three dimensions involved, five π terms would be required. The equation could be written in the following form:

$$\pi_1 = F(\pi_2, \pi_3, \pi_4, \pi_5) \tag{3}$$

It must be emphasized that the only restriction related to the π terms, according to Buckingham Pi Theorem, is that they must be independent and dimensionless.

3. METHODOLOGY

The principal advantage of dimensional analysis is related to a reduction in the number of variables that influence the phenomenon. The key issue is to arrange the parameters in appropriate dimensionless groups. Different sets of data (from every π term) are necessary to describe this process.

In previous studies, similitude was calculated from databases developed using experimental procedures. However, in the present research, not only experimental databases but also numerical databases have been used in order to fit either an exponential or a potential function. The experimental databases used by Nine (1978) were necessary in the final model validation and in the earlier simulations - in this case concerning the FEM model adjustment. Methods were designed with the objective of taking advantage of the positive results obtained from an explicit FEM code to estimate the DBRF.

3.1. Modeling the problem

When a sheet is subjected to the force of the drawbead, a complex combination of geometrical and material factors arises from the deformation forces. Its deformation is complex because the bending of the sheet is inverted four times at punching. Tensile and compressive strains occur, simultaneously, on both sides of the sheet, varying from zero at the neutral axis, to maximum values on the sheet surface. One of the factors which affect the value of these forces is the magnitude of the local strain, according to Nine (1978). This is determined by the geometry of the drawbeads and the thickness of the sheet metal. See Fig. 2:

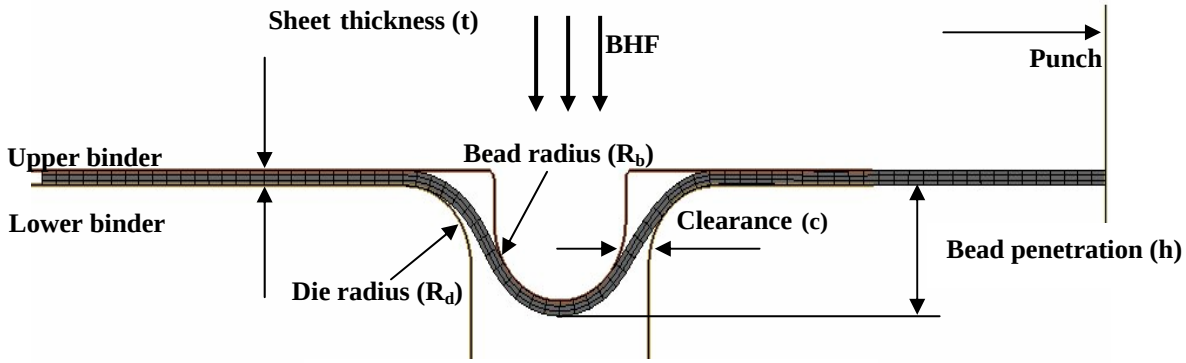

Fig. 2. Circular drawbead parameters.

The deformation forces are also affected by strain hardening, represented by a constitutive equation. Cyclical strain is considerably different from unidirectional increasing strain hardening. Clearance between the blankholder and the drawbeads has an important influence on the observed bending radius. If the observed radius is greater than that used in the reference shape, the bending strain will be less than calculated. It must be remembered that the magnitude of the plastic strain compared to elastic strain will determine the plasticity assumption.

Finally, the strain state may influence the strain hardening. Two FEM models have been designed and their results compared with those obtained from experimental data in order to verify the importance of each of these parameters. This will be explained in the following section.

3.2. Finite Element Models for Achieving Simulation Databases

In order to calculate the most effective DBRF, two different FEM models were designed. In the first, as shown in Fig. 2, a sheet was subjected to a circular drawbead between the upper binder and the die. Its mesh was structured with quadrilateral elements, three of them along the sheet thickness. Figure 2 also demonstrates the blank holding force (BHF) direction, the punch stroke direction and the bead that fits into the die groove.

The second model was designed similarly to the first but without the drawbead, as shown in Fig. 3. The aim was to calculate only the contribution of the drawbead to the DBRF, neglecting the friction effect along the whole of its extension. This contribution is simulated in Model 2 and, subsequently, subtracted from the DBRF calculated in Model 1, with a drawbead.

Twelve independent quantities were chosen to express the relation among nine dimensionless groups, as described in Section 2. Both of these (BHF and DBRF) are shown in Fig. 1. The remaining geometrical forms are available in Fig. 2 as follows: sheet thickness (t), die radius (R_d), bead radius (R_b), clearance (c) and bead penetration (h). The

material properties are taken in account by choosing those parameters assigned: Young Modulus (*E*), Conventional elastic limit (*Sy*), isotropic hardening constant (*K*) and isotropic hardening exponent (*n*), as well as the friction coefficient (μ). After the selection of those parameters which had the most influence on the DBRF, nine π terms were elaborated so that the π Theorem requirements were satisfied.

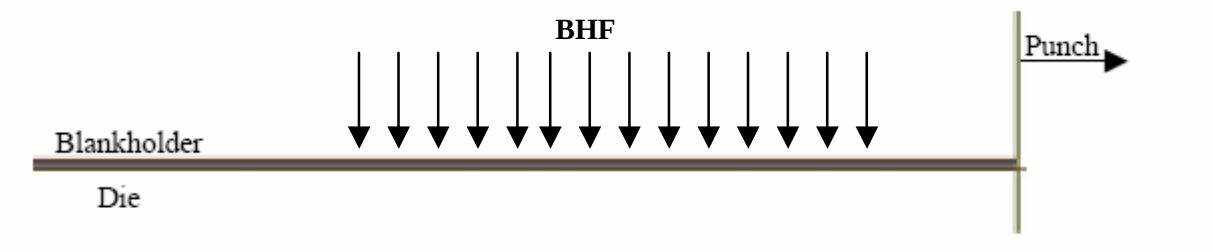

Fig.3. Model 2 with suitable mesh without the drawbead.

In order to reduce the number of necessary phenomenon observations the study variables were arranged in dimensionless groups. However, at least seven data points were identified for each π term from the EF simulations. The value of each parameter was stipulated within a range determined according the most usual values used in practical cases, as following: $\pi_1 = DBRF\ /\ BHF$, is the ratio of restraining force to the blank holding force, both in kN. This π term is the dependent variable in the next relationship which involves the remaining π terms:

$$\pi_1 = F\,(\pi_2, \pi_3, \pi_4, \pi_5, \pi_6, \pi_7, \pi_8, \pi_9) \qquad (4)$$

The others π terms, from Fig. 2, are defined as follows: $\pi_2 = t\ /R_b$ the ratio of sheet thickness (*t*) to the bead radius (R_b), and its range is $0{,}10 \le \pi_2 \le 0{,}35$; Friction coefficient π term μ, $\pi_3 = \mu \le 0{,}30$; Exponent hardening coefficient π term, $\pi_4 = n$, where $0{,}10 \le \pi_4 \le 0{,}30$; $\pi_5 = E/K$, is the ratio of Young Modulus (E) to constant hardening (*K*), $100 \le \pi_5 \le 500$; $\pi_6 = Sy/K$, is the π term that correlates the conventional elastic limit (*Sy*) and the constant hardening (*K*), $0{,}15 \le \pi_6 \le 1{,}20$; $\pi_7 = h/R_b$ is the ratio of bead height (*h*) and the bead radius (R_b), where $0{,}70 \le \pi_7 \le 2{,}50$; $\pi_8 = c/R_b$ correlates the clearance (*c*) and the bead radius(R_b), $0{,}030 \le \pi_8 \le 0{,}300$; $\pi_9 = R_d/R_b$ is the ratio of the die radius (R_d) and the bead radius (R_b), $0{,}30 \le \pi_9 \le 1{,}50$. The values of each parameter were stipulated within a range determined according the most usual values used in practical cases.

The contribution of each parameter for the DBRF must be evaluated. This process was developed by fitting a function to the database which was obtained from FE simulations. At least, seven points for each π term were simulated. To ensure that only the contribution of the parameter under investigation was being evaluated, all simulations were conducted holding the other groups as dimensionless constants with pre estimated values. The chosen functions have the same nature, for fitting the databases were either the potential type, that is $\pi_1 = c_1.(\pi_i)^{c_2}$, or the exponential type, $\pi_1 = c_3.e^{c_4.\pi_i}$

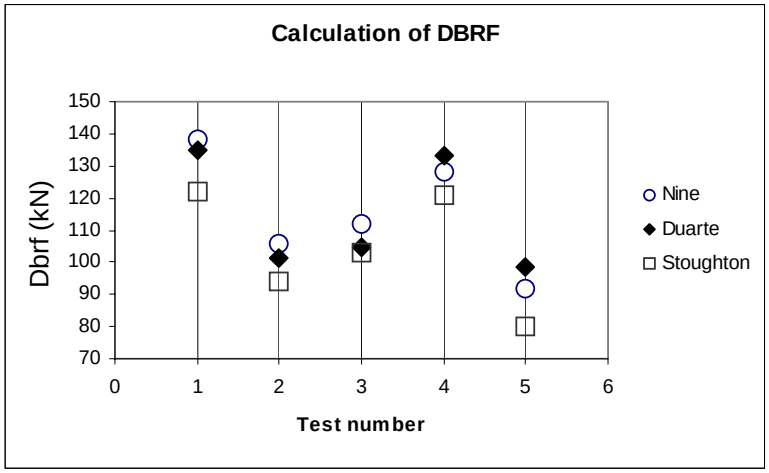

Fig.4. Comparison with analytical and experimental results available in Guo et al. (2000).

By using the proposed approach, it was possible to find an expression in a closed form to estimate the DBRF. These results were compared with Nine's (1978) results and Stoughton's (1988) available in Guo et al. (2000) and are depicted in Fig. 4.

Beyond the mentioned validation procedures, calculations included examination of relative thickness recommended and a perfect fit of the upper bead, without clearances from the die, for both materials. The shoulders, the bead and the die radius were designed with values equal to 4.75 mm. The simulated values for stroke and velocity of the punch were 38 mm and 85 mm/s, respectively. This punch stroke was carefully calculated in order to ensure that a sheet element would pass along the full extension of the drawbead and to simulate the complete process of bending, sliding and unbending the sheet.

Obviously, the precision of the results depends on the accuracy of databases achieved from the simulations. This accuracy also depends on the computational effort spent on each simulation with its explicit solution. Within certain limits it is possible to build a closed formula with a high level of efficiency. For this reason consideration of cost, in terms of time, must be included by the user of this methodology. However, this study is only concerning the influence of geometrical and material parameters on the DBRF.

4. RESULTS AND DISCUSSIONS

As described in the Section 2, the contribution of each parameter for the DBRF must be evaluated. This process has to be developed by fitting a function to the database which was achieved by FE simulations. At least, seven points for each π term must be simulated.

To ensure that only the contribution of the current parameter under investigation is being evaluated, all the simulations are conducted by holding the others dimensionless groups' constants in a pre estimate value. Table 1 shows these used constant values.

Table 1. Constant values adopted in the simulations for the pi terms.

$\overline{\pi}_i$	Constant Dimensionless Groups Used
$\overline{\pi}_2$	$\frac{t}{R_{db}} = \frac{0,76}{4,75} = 0,16$
$\overline{\pi}_3$	$\mu = 0,17$
$\overline{\pi}_4$	$n = 0,23$
$\overline{\pi}_5$	$\frac{E}{K} = \frac{206.000}{516} = 400$
$\overline{\pi}_6$	$\frac{S_y}{K} = \frac{171,7}{516} = 0,33$
$\overline{\pi}_7$	$\frac{h}{R_b} = \frac{7,7}{4,75} = 1,62$
$\overline{\pi}_8$	$\frac{c}{R_b} = \frac{0,76}{4,75} = 0,16$
$\overline{\pi}_9$	$\frac{R_m}{R_b} = \frac{4,75}{4,75} = 1$

To conduct the simulations, the Finite Element (FE) software used was STAMPACK®. The mesh was designed as described in Section 3.

The simulations results are available in Figs. 5 to 12. In every case, for the conditions stipulated in this study, there are the functions which were fitted to the data bases with their correlations, respectively.

Figures 5 and 6 show the results obtained from the simulations for each sheet thickness π term and friction π term, respectively. They were calculated for steel, which has the following material properties: *Sy* = 171.1 MPa, E = 206 GPa and ν = 0.3. These results were obtained after subtracting the Model 2 DBRF from Model 1 DBRF. The figure demonstrates a high correlation between the various thicknesses π term and friction π term values tested with respected to the calculated DBRF: $R^2 = 0.9792$ for sheet thickness π term and $R^2 = 0.9222$ for friction π term. It is still possible to verify the exponentially increases of the DBRF with respect to both π terms.

The results obtained from the simulations for Exponent hardening π term and for Young modulus π term are depicted in the Figs. 7 and 8, respectively. Both figures demonstrate a high correlation between their π terms and the calculated DBRF, that is, $R^2 = 0.9949$ for Exponent hardening π term and $R^2 = 0.9903$ for Young Modulus π term.

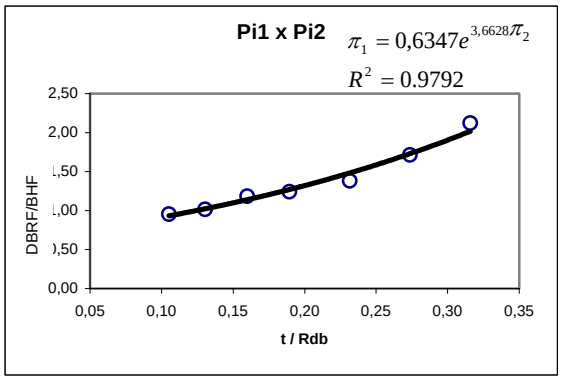

Fig.5. Sheet thickness π term "versus" DBRF.

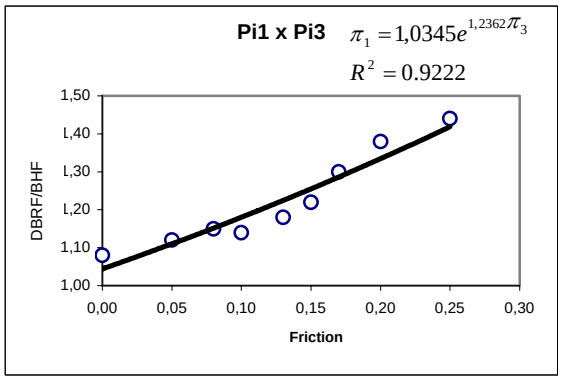

Fig.6. Friction π term "versus" DBRF.

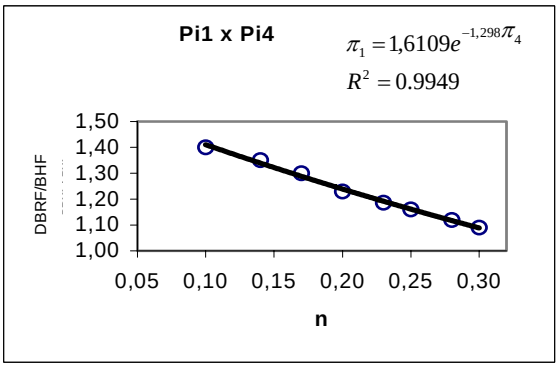

Fig.7. Exponent hardening π term "versus" DBRF

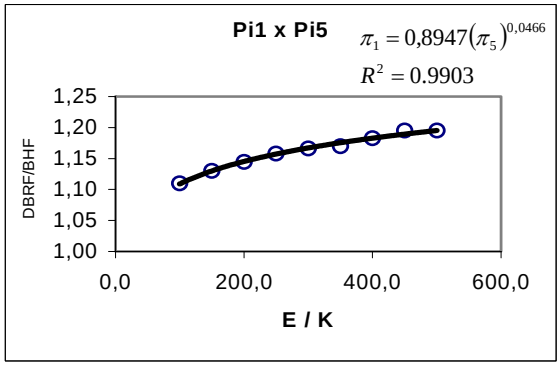

Fig.8. Young Modulus π term "versus" DBRF

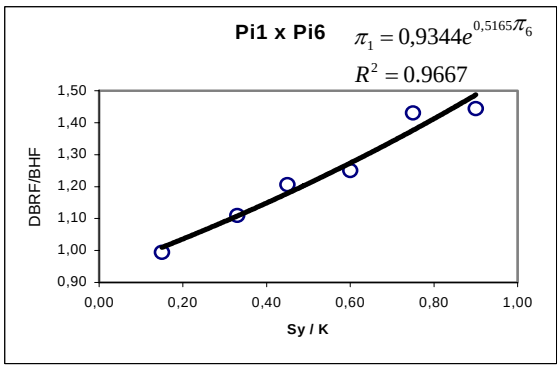

Fig.9. Conventional elastic limit π term "versus" DBRF.

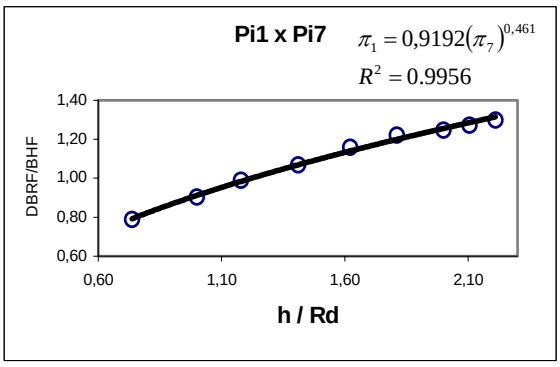

Fig.10. Bead penetration π term "versus" DBRF.

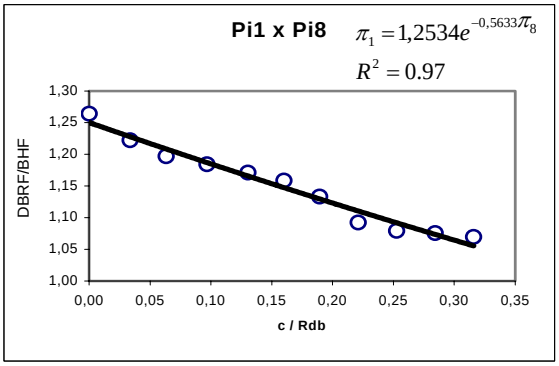

Fig.11. Clearance π term "versus" DBRF.

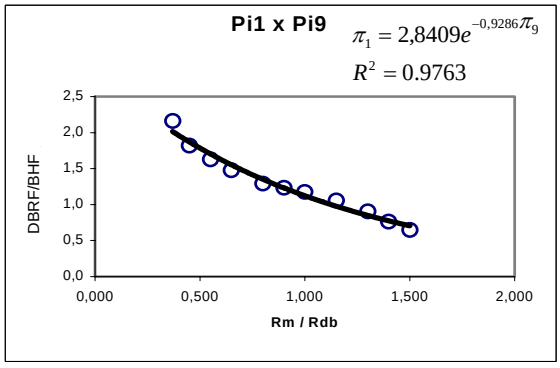

Fig.12. Radii π term "versus" DBRF.

In both Figures, 7 and 8, is possible to verify that the DBRF decreases exponentially with respect to Exponent hardening π term and increases potentially with respect to Young modulus π term.

The same thing happens with Clearance π term and Radii π term with respect to DBRF which decreases exponentially with very good correlations, that is, $R^2 = 0.9700$ and $R^2 = 0.9762$, respectively. This may be verified in Figs. 11 and 12.

The behavior of DBRF with respect to Conventional elastic limit π term and to Bead penetration π term are similar, that is, there are exponentially increases of the DBRF, in Figs 9 and 10, with respect to both π terms. There are high correlations between the various Bead penetration π term values tested and the calculated DBRF: $R^2 = 0.9667$ for Conventional elastic limit π term and $R^2 = 0.9956$ for Bead penetration π term.

Input output scatter plots are in general a very simple and informative way of running a sensitivity analysis. Once plotted on a common scale for DBRF "versus" some π term, for example, these plots provide for an immediate appreciation of which parameters has more influence on the restraining force parameter.

Using the above procedure is possible to see that the Sheet thickness π term has the greater influence on the DBRF and the Young Modulus π term is the smallest one in terms of influence on the DBRF. The others have intermediate values between them.

5. CONCLUSIONS

Two FE models were designed to simulate a sheet metal forming process considering the contributions of eight dimensionless groups on the DBRF - drawbead restraining force.

In every case a function was fitted, using the methodology proposed: use of similitude in engineering with FE simulation data bases to determine the influence of material and geometrical parameters on the circular DBRF.

Predictions made in this study have were contrasted to 2D FE simulations carried out with STAMPACK®, with experimental data bases of Nine (1978) and with the analytical model of Stoughton (1988).

The average of absolute error with respect to experimental data bases was about 6 % and, for the cases studied, the maximum discrepancy was found to be less than 10%.

Predictions derived from this approach are adequate, in terms of precision, when compared with the analytical model of Stoughton (1988) because the average of absolute error was about 5 % and, for the cases studied, the maximum error was approximately 7%.

Furthermore, evaluations with this approach were considered adequate, in terms of precision, when compared with 2D FE simulations carried out with STAMPACK®. In these contrasts, the maximum discrepancy was found to be less than 10%.

For this reason, the approach was used to develop a study about DBRF evaluations and was accepted as a contribution by STAMPACK®, an explicit finite element code used to simulate the forming process.

6. ACKNOWLEDGEMENTS

As a doctoral student of the Federal University of Uberlândia, Duarte, E. N. wishes to acknowledge the support of CAPES - Coordenação de Aperfeiçoamento de Pessoal do Ensino Superior, of the Ministry of Education of Brazil.

The authors also thank the Quantech ATZ, the Red de Aulas CIMNE in Barcelona, Spain, the Instituto Fábrica do Milênio, in Brazil and the Professor Ph.D. David Francis George for the English correction.

7. REFERENCES

Carleer, B.D., P.T. Vreede, P. Drent, M.F.M. Louwes and J. Huetink, (1995), " Modeling Drawbeads with Finite Elements and Verification", J. Mater. Process. Technol., Vol. 45, pp. 63-68.

Duarte, E., Oliveira, S A. G (2005), "The Influence of the Sheet Thickness on the Drawbead Restraining Force",Proceedings of the 18th Brazilian Congress of Mechanical Engineering, Vol.1, Ouro Preto, Brazil.

Guo, Y.Q., Batoz, J.L., Naceur, H., Bouabdallah, S., Mercier, F., Barlet, O., "Recent Developments on the Analysis and Optimum Design of Sheet Metal Forming Parts Using a Simplified Inverse Approach", J. Computers and Structures; 78, 133-148 (2000).

Levy, B.S. (1983), "Development of a Predictive Model for Draw Bead Restraining Force Utilizing Work of Nine and Wang", J. Applied Metalworking, 3(1), pp. 38-44.

Murphy, G. (1950) "Similitude in Engineering", pp. 17-47, The Ronald Press Co., N.Y., USA. NAFEMS (1992), "Introduction to Nonlinear Finite Element Analysis". Ed. By E. Hinton, 1st ed.. East Kilbride,Glasgow.1992 .

Nine, H. D., (1978) , "Drawbead Forces in Sheet Metal Forming", in: D. P. Koistinen, N. M. Wang (Eds.), Mechanics of Sheet Metal Forming, Plenum Press, N. York, 1978, pp.179-211.

Stoughton, T. B., (1988), "Model of Drawbead Forces in Sheet Metal Forming", Proc. 15th Biennial Congress of IDDRG, May 18-21, Dearborn, MI, pp. 205-215.

STAMPACK®, (2003), "Theory Manual", v. 54. Quantech ATZ S.A. Barcelona, Spain. Swift, M. A. (1948), Engineering, 166, 333.
Tufekci, S.S., Wang, C.T., Kinzel, G.L, and Altan, T., (1994), “Estimation and Control of Drawbead Forces in Sheet Metal Forming“, SAE Paper No. 940941.